Algal Research 84 (2024) 103759

Contents lists available at ScienceDirect

Algal Research

journal homepage: www.elsevier.com/locate/algal

Pilot plant cultivation of microalga *Dictyosphaerium chlorelloides* with night illumination from LEDs sources

Jana Kvíderová [a,b,c,*], David Kubáč [d], Jaromír Lukavský [a]

[a] Academy of Sciences of the Czech Republic, Institute of Botany, Department of Phycology, Dukelská 135, 378 01 Třeboň, Czech Republic
[b] University of South Bohemia in České Budějovice, Faculty of Sciences, Center for Polar Ecology, Na Zlaté stoce 3, 370 05 České Budějovice, Czech Republic
[c] University of Western Bohemia, Faculty of Education, Klatovská 51, Plzeň, Czech Republic
[d] Algatech Třeboň, Opatovický mlýn, Czech Republic Academy of Sciences of the Czech Republic, Czech Republic

ARTICLE INFO

Keywords:
Pilot-plant mass cultivation
Microalga
Dictyosphaerium chlorelloides
LEDs
Night lighting
Extracellular polysaccharides

ABSTRACT

Illumination during the night with white LEDs increased the growth of the microalga *Dictyosphaerium chlorelloides* strain CCALA 330 on a thin-film platform unit (150 L volume, 12 m^2 area) approximately 2.5× in comparison to the platform illuminated only by the Sun. The mean PAR intensity on the Sun-illuminated unit was 71 μmol m^{-2} s^{-1}, on the Sun + LEDs unit 549 μmol m^{-2} s^{-1}, the mean temperatures were 15 °C and 20.1 °C. On the Sun unit the algae grew to a maximum of 15 g L^{-1} dry weight in 42 days, with Sun + LEDs into 17.8 g L^{-1} during 24 days when the both units reached the stationary phase of the growth curve. Biomass production was 3.3 in the Sun and 8.54 g m^{-2} d^{-1} in the Sun + LED, i.e. 0.27 and 0.68 g L^{-1} d^{-1}. In total, the mean of 37.5 and 58.2 kWh per night were consumed, so the total electricity consumptions for biomass production was 0.20 and 0.40 kWh g^{-1} DW during LED + Sun cycles 1 and 2, respectively. The production of the extracellular polysaccharides was practically the same for both platforms, and constant during time. A more substantial double increase was only after 30 days of cultivation in both platforms and reached 4 g L^{-1}. The fluorescence measurements proved good physiological state of the cultures. The PAR was found as a main driver of the photosynthetic activity. The correlation of the growth and fluorescence parameters to the environmental conditions was much more profound in the Sun pilot plant, therefore the reliable set of monitored parameters should be defined according to the cultivation type, for both of them we propose OD_{680}/OD_{720} ratio as a proxy of nutrient deficiency.

Abbreviations: AGR, absolute growth rate; DW, dry weight; DW_{max}, maximum DW content; DW_{min}, minimum DW content; EPSs, extracellular polysaccharides; F_M/F_0, ratio of maximum (F_M) and minimum (F_0) fluorescence; F_S, steady-state fluorescence in light; F_V/F_0, ratio of variable (F_v) and minimum (F_0) fluorescence; F_V/F_M, maximum quantum yield in dark; J_0^{ABS}/RC, average absorbed photon flux per active reaction center; J_0^{DI}/RC, energy flux dissipated as heat; J_0^{ET2}/RC, electron transport flux from Q_A to Q_B per active center; J_0^{RE1}/RC, electron transport flux to photosystem I electron acceptor per active center; J_0^{TR}/RC, maximum trapped electron flux per active center; L/D, light/dark; LED, light emitting diode(s); M_0, maximum rate of accumulation of closed RCs at the beginning of fluorescence rise; OD_{680}, optical density was measured at 680 nm, chlorophyll *a* proxy; OD_{720}, optical density was measured at 720 nm, dry weight proxy; OD_{750}, optical density was measured at 750 nm, dry weight proxy; PAR, photosyntetically active radiation (400–700 nm); rETR, relative electron transport rate; t_{Fmax}, time necessary to reach the fluorescence maximum; T_{air}, air temperature; $T_{suspension}$, suspension temperature; V_J, normalized fluorescence intensity at 2 ms (J-step); V_I, normalized fluorescence intensity at 60 ms (I-step); δ, efficiency/probability that electron trapped by PSII will be transferred from Q_B to photosystem I electron acceptor; μ, relative growth rate; φ_{Po}, maximum quantum yield of primary photochemistry of photosystem II; φ_{ET2o}, quantum yield of electron transport flux from Q_A to Q_B; φ_{RE1o}, quantum yield of electron transport flux to photosystem I electron acceptor; φ_{Do}, quantum yield of energy dissipation; Φ_{PSII}, effective quantum yield in light; Ψ_{ET2o}, efficiency/probability that electron trapped by photosystem II will be transferred to Q_A; Ψ_{RE1o}, efficiency/probability that electron trapped by photosystem II will be transferred to photosystem I electron acceptor.

* Corresponding author at: Academy of Sciences of the Czech Republic, Institute of Botany, Department of Plant Ecology, Dukelská 135, 378 01 Třeboň, Czech Republic.

E-mail address: jana.kviderova@objektivem.net (J. Kvíderová).

https://doi.org/10.1016/j.algal.2024.103759
Received 2 May 2023; Received in revised form 26 July 2024; Accepted 15 October 2024
Available online 19 October 2024

1. Introduction

Microalgae are intensively studied as the source of biomass, oils, pigments, vitamins, biologically active substances, etc., e.g. Borowitzka, Pulz et Gross, Perosa et al. [1–3]. To maximize the yields of the biomass and/or high-value compounds, the optimalization of the cultivation process is necessary, and its fast autonomous regulation of is required, as well as the minimalization of the costs for commercialization of the products.

Light regime, i.e. light period duration, light intensity and light color, is one of the most important factors affecting the algal growth and productivity. The LED light sources allow precise regulation of the light regime, and have been applied in algal research since mid-90ties of the 20th century [4]. So far, LED lights have been used almost exclusively for small-scale cultivation in laboratory scale, e.g. Nedbal et al. [5] and in medium- and large-scale closed cultivation systems, e.g. Sergejevová et al., Glemster et al. [6,7]. Contrary to the large closed cultivations, the LED light sources are not used frequently in the open cultivation units [8] and the Sun represents the only light source. Hence, the nocturnal losses of biomass by respiration could reach about 5–8 % of the biomass, depending on temperature, growth curve phase, suspension density, and oxygen supply at night [9]. Therefore, continuous operation of the photobioreactor, where light is supplied by the Sun during the day and LED light sources at night, should eliminate losses during night respiration with minimal costs and increase the biomass yields compared to continuous LED illumination [8]. Moreover, the night LED illumination could extend the cultivation period to winter in temperate regions and in summer in the Polar Regions at the end of the vegetative season [10].

According to Blanken et al. [11], the cost of biomass production doubles if the light source is only LED lamps and it is realistic to use them only in the production of valuable materials such as astaxanthin. However, data and experience with LED + Sun illumination at least on a medium and large pilot scale are still lacking for microalgae, as the only similar experiments were focused on simulation the Mediterranean climate and light for desired end product of lipids in the -marine microalga *Microchloropsis salina* in artificial seawater [8], and even in such case, energy consumption and economical calculations were not performed.

Beside the LED illumination in open thin-layer units, determination of the crucial parameters that may be used for autonomous operations of open pilot plants represents a novel challenge in algal cultivation. Such measurements should be fast, easy and include biomass content as well as the monitoring of the physiological state of the culture. The biomass could be, and regularly is, evaluated using standard spectrophotometric parameters, i.e. optical densities at 750/720 nm as biomass proxy and optical density at 682/680 nm as chlorophyll *a* proxy (e.g. Andersen [12] and the physiological state by variable chlorophyll fluorescence methods (e.g. Masojídek et al., Malapascua et al. [13,14]. Although the variable chlorophyll fluorescence has been applied in algal mass cultivations to determine optimum and sub-optimum conditions in laboratory and mass cultivations [14–18], no continuous automatic fluorescence monitoring was performed in open pilot plant conditions so far, especially in lower (i.e. below 20 °C) temperatures. Recent development of simple hand-devices for spectrophotometric and fluorometric measurements could extend these measurements to the industrial production. Reliable set of spectrophotometric and fluorometric parameters defining the actual algal growth should be established for routine applications.

For cultivation in colder part of the year in the temperate zone (spring, fall) to evaluate the efficiency of LED illumination and definition of suitable monitoring parameters, the green alga *Dictyosphaerium* seems to be a perspective alga due to its good growth at temperatures around 20 °C and at relatively low irradiances [19–21]. Our experimental strain *Dictyosphaerium chlorelloides* CCALA 330 growth optimum temperatures ranged from 15 to 20 °C and irradiances up to 50 μmol m^{-2} s^{-1} and maximum EPS production at temperatures around 25 °C and irradiances around 50 μmol m^{-2} s^{-1} [19], so upscaling of the cultivation to 150 L during colder part of the year is inevitable for future commercialization. This alga is also able to produce large amounts of extracellular polysaccharides (EPSs), sometimes the culture thickens to the consistency of agar [22]. The EPSs of microalgae are very diverse and belong to a group of the high-value compounds searched for, as they show wide spectrum of biological activities [23], important for, e.g. biomedical applications [24,25] or waste water treatment [22,26]. The *Dictyosphaerium chlorelloides* EPSs are promising in terms of their biological activity; many of them have shown antibacterial, antiviral and anticarcinogenic effects [27–30].

The aims of the study are (a) to verify the increase in the production of biomass and ECP *Dictyosphaerium chlorelloides* during only the night illumination of the open, thin layer large-scale photobioreactor with an additional LED light source (b) to perform basic energy consumption and economic estimation of LED illumination for biomass and EPS production, and (c) to determine suitable spectrophotometric and fluorescence parameters for biomass and physiological state autonomous monitoring during cultivation.

2. Material and methods

2.1. Strain and inoculum preparation

The microalga strain *Dictyosphaerium chlorelloides* CCALA 330 was pre-cultured in 2 L bottles at room temperature (22–25 °C) and in continuous light of irradiance about 100 μmol.m^{-2}.s^{-1} (Optonica LED panel light DL2358, Bulgaria). The 1/2SŠ medium [31] was continuously aerated with an excess of a mixture of air and CO_2 around 2 %. After 3 weeks, the inoculum was transferred to a thin-film pilot plant platform, in total inoculum volume of about 10 % of total volume of the pilot plant to achieve sufficient cell density above the detection limits of used spectrophotometers and fluorometers for reliable measurements with high signal-to-noise ratio, especially for continuous variable chlorophyll fluorescence monitoring (Section 2.5.1) and fluorescence transient measurements (Section 2.5.3).

2.2. Large-scale photobioreactor cultivation

Two identical thin-layer flat platforms of the area of 12 m^2, of volume of 150 L and of a surface/volume ratio of 80 [32] according to Doucha et Lívanský [33] were placed in a greenhouse without tempering. The lighting of one of them was equipped by 24 pieces of LED panels (further referred as LED + Sun pilot plant; see Section 2.3 for detailed information) hung above the platform, in two rows, reducing thus shadowing of sunshine by the light source during day (Fig. 1). For comparison, the second platform was illuminated only by the Sun during the daytime and as "night" was considered time interval between sunset + 30 min and sunrise − 30 min; the 30-minute interval was based on rules for visual regime of flight (further referred as the Sun pilot plant).

Both platforms were equipped with data loggers Minikin QTi datalogger to record air temperature (T_{air}) and photosyntetically active radiation (PAR; 400–700 nm), and Minikin Tie to record suspension temperature ($T_{suspension}$) (EMS Brno, CZ). The data were recorded in 10 min intervals.

Contrary to inoculum cultivation, the 1/2SŠ medium [31] was prepared from tap water by pouring in the appropriate chemicals, without sterilization. The illuminated platform was inoculated first, then after 4 days of growth, half of the suspension was transferred to the second platform and the volumes were supplemented with tap water and nutrients to get homogenous inoculum for both platforms with the same history of acclimatization to new cultivation conditions, i.e. large suspension volume, temperature and light variation, circulation regime with mechanical stress due to pumping and slightly different medium composition due to use of tap water.

The CO_2 was supplied at a rate of approx. 5 L min^{-1} into front of the

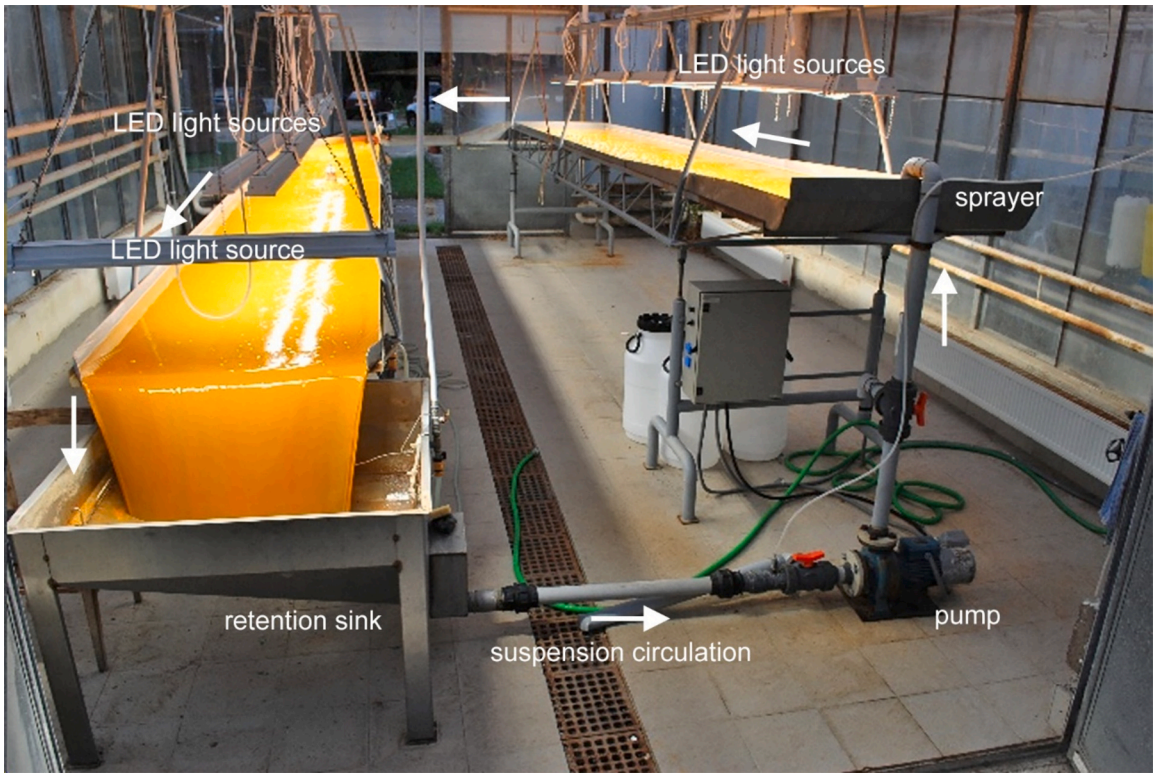

Fig. 1. The experimental pilot plant according to Doucha et Lívanský [33] with LED light sources during night.

pumps, on the Sun platform only during the day.

The feedback regime (in fact semi-continuous regime) when the volume of the inoculum is considered) was tested on the illuminated platform, after reaching the stationary phase of the growth curve, the suspension was harvested. Water and nutrients were added, and another phase was started without new inoculation. The remnants of the suspension on the platform, in the circulation system and the pump served as an inoculum.

2.3. LED light sources

The OptimaLED 134W (Thome Lightning, Czech Republic; Fig. 1), with Digital Adressable Lighting Interface (DALI), are white, daylight, thin longitudinal LED panels providing little shade and allow the platform to be illuminated by the Sun during the day. Small lenses in front of point sources focus the light exactly on the surface of the unit. At the intensity of the Sun below and above 5 μmol m^{-2} s^{-1}, the LED panels are switched on and off automatically by a twilight switch (Cd-DALI/DSI, BEG Brück Electronic GmbH, Germany). The expected intensity of the LED lights should reach the level of the cultivation area almost 1000 μmol m^{-2} s^{-1}. The nominal power consumption of one panel was 98 W.

2.4. Biomass production

The cultivation in both units lasted from September 4 to November 20, 2020. Each day, the optical density was measured at 750 nm (OD_{750}; Shimadzu UV-1600 spectrophotometer, Shimatzu, Japan), as well as the photosynthetic capacity by the method described in sections. The dry weight (DW) was measured gravimetrically at 2 day intervals by pipetting 2 mL into a pre-weighed Eppendorf tube, centrifuged at 1000*g* for 20 min, the supernatant slit, and the biomass was dried at 105 °C in hot air dryer to reach constant biomass weight. In parallel, similar measurements were performed using handheld fluorometer AquaPen AP 110-C (A-pen; Photon Systems Instruments, CZ) where the optical density was measured at 720 (OD_{720}; dry weight) and 680 (OD_{680}; chlorophyll *a*) nm. The conversion equations were derived from dilution series and biomass and chlorophyll content were determined according to Kvíderová et Henley [34].

The growth of the culture during entire cultivation was characterized by the 4-parameters logistic curve fitting

$$DW\left[g\,L^{-1}\right] = DW_{min} + \frac{DW_{max} - DW_{min}}{1 + \left(\frac{t}{t_i}\right)^{S}} \quad (1)$$

where DW_{min} is minimum DW content, DW_{max} is the maximum DW content, t is cultivation time in days, t_i is the time when curve inflection occurs, and S is curve slope. The absolute growth rate (AGR) was calculated from the first derivation of the Eq. (1) for t_i as

$$AGR\left[g\,L^{-1}\,d^{-1}\right] = \frac{S \times (DW_{min} - DW_{max})}{4 \times t_i} \quad (2)$$

For the estimation of relative growth rate (μ), the dry weight data were ln-transformed.

The 2-parameters exponential function was used to fit the initial phase of the cultivation

$$DW\left[g\,L^{-1}\right] = DW_{min}e^{\mu t} \quad (3)$$

where DW_{min} is minimum DW content, t is cultivation time in days, and μ is the relative growth rate in d^{-1}.

Finally, the ratio of the OD_{680} and OD_{720} (OD_{680}:OD_{720}) was calculated for AquaPen spectrophotometric measurements as

$$OD_{680} : OD_{720} = \frac{OD_{680}}{OD_{720}} \quad (4)$$

And similarly, the ratio of Chl *a* and DW (Chl *a*: DW) was calculated as

$$Chl\ a : DW\left[mg\ g^{-1}\right] = \frac{Ch\ a}{DW} \quad (5)$$

where the Chl *a* is the Chlorophyll a concentration in mg L^{-1} and DW is the dry weight content in g L^{-1} to reveal possible nitrogen limitation [35,36].

2.5. Photosynthetic activity measurements

2.5.1. Continuous photosynthetic performance monitoring

The actual photosynthetic performance was estimated from the measurements of the effective quantum yield (Φ_{PSII}) by Monitoring Pen MP 100-E (M-pen; Photons Systems Instruments, CZ). Each pilot plant was equipped by one M-pen. The Φ_{PSII} was measured in 15 min intervals. The relative electron transfer rate (rETiR) was calculated according to Maxwell et Johnson [37]. When necessary, the outliers were detected using running mean method with centered window, and were filled using linear interpolation.

2.5.2. Maximum quantum yield

The maximum quantum yield (F_V/F_M) used for estimation of the physiological state of the photosynthetic (micro)organisms was measured using AquaPen AP 110-C (Photon Systems Instruments, CZ). The F_V/F_M was measured after 15 min dark adaptation. The F_V/F_M was calculated according to Roháček et al. [38].

2.5.3. Fluorescence transient

The fluorescence transient (OJIP transient) used for estimation of the physiological state of the photosynthetic (micro)organisms was measured using AquaPen AP 110-C (Photon Systems Instruments, CZ). The OJIP transient was measured after 15 min dark adaptation. The OJIP transient parameters were calculated according to Stibert et al. [39] and Strasser et al. [40]. The used OJIP parameters and their physiological meaning are summarized in Supplementary material 1.

2.6. Extracellular polysaccharides

The EPSs content was determined by weighing the dried biomass of pre-weighed 2 mL Eppendorf tubes where the supernatant from the first one was poured into the second one and both were slowly dried to 105 °C and weighed.

2.7. Statistics

The microclimate descriptive statistics calculation and comparison between the pilot plants were performed using Statistica 13.2 software. The outliners selection and curve fittings were performed using Matlab SW 2021a©. The multivariate analyses were performed using CANOCO 5.0 software [41]. The results were considered statistically significant for $P < 0.05$.

Table 1
The detailed microclimate characteristics during cultivation, comparison of conditions during parallel cultivation and biomass yield and productivity in Solar + LED and Solar pilot plant. The statistical significance of differences was evaluated by paired *t*-test. The statistically significant differences are marked in bold. Abbreviations: *n* – number of observations, CET – Central European Time, s.d. – standard deviation.

	Sun + LED unit				Sun unit	Comparison		Statistical significance	
	Cultivation total	Pre-cultivation	LED + Sun 1	LED + Sun 2	Sun	ĹED + Sun unit	Sun	t-Value	*P*-value
Start [CET]	1.9.2020 8:10	1.9.2020 8:10	4.9.2020 8:00	30.9.2020 6:20	4.9.2020 8:00	4.9.2020 8:00	4.9.2020 8:00		
End [CET]	3.11.2020 7:30	4.9.2020 8:00	30.9.2020 6:20	3.11.2020 7:30	20.11.2020 11:10	3.11.2020 8:00	3.11.2020 8:00		
Cultivation duration [d]	63	3	26	35	78	60	60		
Final volume of suspension [L]		150	150	150	150	150	150		
Area of the unit [m^2]		12	12	12	12	12	12		
Cultivation conditions									
Number of cases [max]	9081	433	3734	4906	11,108	8638	8638		
Air temperature									
Mean ± s.d. [°C]	23.2 ± 5.2	26.9 ± 5.1	26.0 ± 5.2	20.8 ± 3.8	16.3 ± 6.8	23.0 ± 5.1	17.7 ± 6.8	**115.92**	**<0.001**
Median [°C]	22.7	26.1	25.9	20.8	14.5	22.5	16.1		
Minimum [°C]	8.8	14.5	13.0	8.8	5.3	8.8	5.3		
Maximum [°C]	40.5	40.5	40.4	38.9	41.6	40.5	41.6		
Suspension temperature									
Mean ± s.d. [°C]	20.5 ± 3.8	17.1 ± 3.7	22.5 ± 3.8	18.9 ± 2.9	15.5 ± 5.3	20.4 ± 3.8	16.8 ± 5.2	**131.26**	**<0.001**
Median [°C]	20.2	16.9	21.8	18.7	14.4	20.1	15.9		
Minimum [°C]	9.9	16.3	14.8	9.9	5.6	9.9	5.6		
Maximum [°C]	33.0	19.4	31.2	31.7	31.5	33.0	31.5		
Irradiance									
Mean ± s.d. [μmol.m^{-2}.s^{-1}]	552 ± 394	634 ± 411	542 ± 383	554 ± 401	60 ± 115	549 ± 393	71 ± 127	**95.48**	**<0.001**
Median [μmol.m^{-2}.s^{-1}]	816	966	706	833	0	815	0.2716		
Minimum [μmol.m^{-2}.s^{-1}]	1	5	1	4	0	1	0		
Maximum [μmol.m^{-2}.s^{-1}]	1242	1242	1009	983	1307	1009	1307		
Diel sum of radiation									
Mean ± s.d. [MJ.m^{-2}.d^{-1}]	10.28 ± 0.92	6.68 ± 4.07	9.85 ± 1.50	10.20 ± 1.34	1.12 ± 0.81	10.20 ± 1.09	1.32 ± 0.80	**50.95**	**<0.001**
Median [MJ.m^{-2}.d^{-1}]	10.45	9.32	10.20	10.62	0.88	10.37	1.08		
Minimum [MJ.m^{-2}.d^{-1}]	4.84	0.02	4.65	4.82	0.14	4.82	0.00		
Maximum [MJ.m^{-2}.d^{-1}]	11.38	10.69	11.36	11.38	2.82	11.38	2.82		
Total sum of radiation during cultivation [MJ.m^{-2}]	658.22	36.02	265.58	356.61	87.24	622.20	80.39		
Biomass production									
Total produced biomass [dry weight, g]	6150		2700	3450	2400	6150	2400		
Mean daily biomass production per area [g DW.m^{-2}.d^{-1}]	8.135		8.654	8.214	2.564	8.542	3.333		
Mean daily biomass production per suspension volume [g DW.L^{-1}.d^{-1}]	0.651		0.692	0.657	0.205	0.683	0.267		

3. Results

3.1. Microclimate in the pilot plants

Two complete cultivation cycles, i.e. reaching the stationary phase, were performed in the LED + solar pilot plants (LED + Sun 1 and LED + Sun 2), and one in the solar pilot plant (Sun) were performed between September 4–November 20, 2020 (Table 1). The courses of T_{air}, $T_{suspension}$ and PAR during cultivation showed distinct differences between the pilot plants (Fig. 2).

The microclimate comparison performed for data collected between 4.9.2020 8:00 and 3.11.2020 8:00 CET showed that the Solar + LED pilot plant had been significantly warmer by than Solar pilot plant (Table 1). The mean T_{air} and $T_{suspension}$ were higher in the LED pilot plant by 5.3 and 3.6 °C, the T_{air} and $T_{suspension}$ minima by 3.5 °C and 4.3 °C, respectively. Surprisingly, the T_{air} maximum was lower by 1.1 °C in the LED pilot plant, while $T_{suspension}$ maximum was higher by 1.5 °C. Mean irradiance was 7.73× higher than at the Solar plant. However, when the daytime was considered (8:00–16:00 to avoid the interference of LED illumination), the mean irradiance was by 23 % higher at the solar pilot plant due to LED panel shielding (paired t-rest, $n = 2940$, t-value = −20.90, $P < 0.001$). The total sum of radiation received during cultivation was 7.74× higher than in the Solar plant (Fig. 3). However, the total sum of radiation received during daytime (8:00–16:00) was by 24 % higher at the Solar plant (paired t-rest, $n = 59$, t-value = −10.89, $P < 0.001$; Supplementary material 2).

The diel courses were different for both pilot plants. In the LED + Sun pilot plant, the T_{air} and $T_{suspension}$ were more stable, especially during night-time. Both temperatures declined steeper after switching the LED illumination off (Supplementary material 3). The PAR provided relatively stable illumination during night-time, however the daytime PAR maxima reached comparable irradiance only once, and for short period of time (Fig. 4). The PAR in the solar pilot plant reached the values comparable to LED illumination several times (Fig. 4).

The suspension temperature was found to be independent of PAR in the cultivations with LED illumination (LED + Sun 1: $n = 2369$, $r = -0.0701$, $P = 0.001$; LED + Sun 2: $n = 3246$, $r = 0.0158$, $P = 0.367$), while these environmental variables were strongly positive correlated in sun pilot plant ($n = 5611$, $r = 0.6936$, $P < 0.001$).

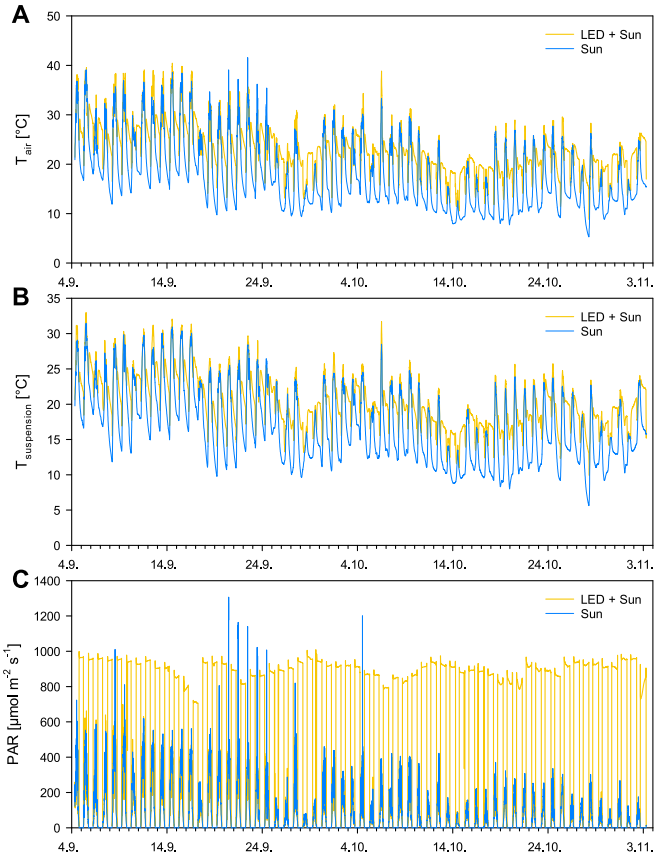

Fig. 2. The courses of (A) air temperature (T_{air}), (B) suspension temperature $T_{suspension}$) and (C) photosynthetically active radiation (PAR) during *Dictyosphaerium chlorelloides* CCALA 330 cultivation on September 4–November 11, 2020 when simultaneous LED and control cultivations were performed.

3.2. Algal cultivation in the large-scale photobioreactor

3.2.1. Algal growth in the pilot plant units

The LED night illumination increased biomass production significantly (Fig. 5 and Table 2). The highest DW content was produced in the first cultivation cycle (LED + Sun 1). During the second cultivation cycle, the biomass production was slightly lower, but still much higher than in the solar pilot plant. Although the differences in the μ were not found significant, the AGR was the highest in the LED + Sun cycle 1 than in the LED + Sun cycle 2 and the AGR in the solar plant was the lowest during the first 15 days of cultivation (Table 2). Since after 15 days the μ and AGR were similar, the first 15 days were probably crucial for the final biomass production (Supplementary material 4).

Since the duration of the cultivation differed among the cultivation cycles, i.e. 26, 35 and 78 days for LED + Sun 1, LED + Sun 2 and Sun cycles, respectively, the growth curves were fitted by the logistic curve (Fig. 5). The parameters revealed similar maximum DW content in the LED + Sun cycles which was higher than in the Sun cycle. The DW_{max} during real cultivation were higher, as they reflect variability during the stationary phase (Table 2).

However, the μ and AGR values were higher in the LED + Sun 1 cycle that in the LED + Sun 2 cycles, and the growth rates in both LED + Sun cycled were higher than in the Sun cycle. The exponential function fitting estimated higher growth rates than logistic function fitting since the logistic curve covers entire cultivation. The estimated μ and AGR values corresponded to real data during the first five to ten days of cultivation (Supplementary materials 4 and 5).

The Chl *a* content followed the dry weight content, however, the Chl *a* concentrations were comparable in both light regimes. The nutrient additions LED + Sun 2 and Sun batches led to rise of the Chl *a* content (Fig. 6). The highest values were observed during the LED + Sun 2 cultivation. The growth rates based on Chl *a* were higher in the LED + Sun 1 cultivation (Supplementary material 6).

The OD_{680}:OD_{720} ratio, and hence Chl *a*: DW ratio, were higher in the solar pilot plant in general (Fig. 7, Table 3; OD_{680}:OD_{720} Kruskal-Wallis ANOVA, H = 21.22, $P < 0.001$; Chl *a*: DW ratio Kruskal-Wallis ANOVA, H = 25.34, $P < 0.001$). The course was similar in all batches. The initial steep rise was followed by slower decline, approaching 1 in late phase of cultivations. The peaks of the ratio occurred on 2nd, 3rd and 4th days in LED + Sun 1, LED + Sun 2 and Sun cultivation cycles. The nutrient additions in later phases of cultivations led to the sudden increase again (Figs. 6, 7). The values of the OD_{680}:OD_{720} ratio were strongly positive correlated in individual batches (LED + Sun 1: $r = 0.9965$, $P < 0.001$; LED +Sun 2: $r = 0.9296$, $P < 0.001$; Sun: 0.9826, $P < 0.9826$) as well as if all data were evaluated together ($r = 9786$, $P < 0.001$) (Supplementary material 7).

3.2.2. The biomass production and electricity consumption

Total of 2700, 3450, and 2400 g of *D. chlorelloides* DW was produced in the LED + Sun 1, LED + Sun 2 and in the Sun cultivation cycles, respectively (Table). The LED + Sun illumination resulted in total production of 6150 g of DW, 2.5× higher that in Sun illumination, indicating thus additional LED illumination as important energy source for growth. The total energy consumption reached 1013.7 kW, and the consumption was higher due to longer nights during the LED + Sun 2

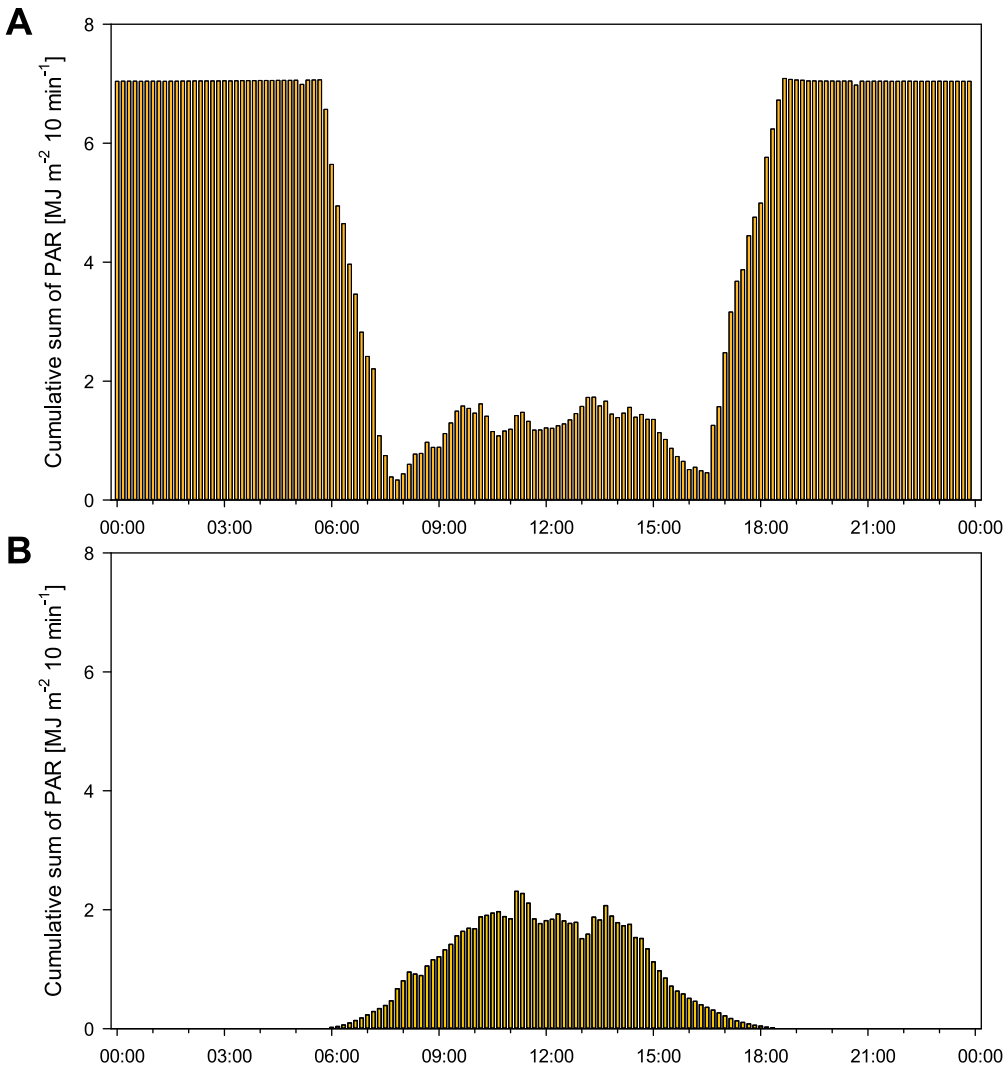

Fig. 3. Cumulative sum of PAR during parallel cultivation in (A) LED + Sun and (B) Sun pilot plants during one day.

cycle (Table 4).

3.2.3. *Comparison of the spectrophotometric methods to track the algal growth*

The three spectrophotometric parameters, OD_{750} measured by a standard bench spectrophotometer, OD_{720} and OD_{680}, both measured by a handheld spectrophotometer/fluorometer, were significantly strongly positively correlated, especially between OD_{750} and OD_{720} used as a biomass proxy (Supplementary material 8). Therefore, the data based on optical densities measured by a standard bench spectrophotometer and handheld spectrophotometer/fluorometer were considered as complementary. The fluorometric parameter F_S (diel mean) measured by a monitoring fluorometer was also significantly positively correlated to spectrophotometric parameters, but this dependence was weaker (Supplementary material 8).

3.3. *Physiological performance*

3.3.1. *Photosynthetic performance*

The record of the variable chlorophyll fluorescence measurements revealed peaks in the steady-state fluorescence in light (F_S) related to sudden decrease of the effective quantum yield (Φ_{PSII}) due to pilot plant maintenance. These outlying datapoints were cleaned for further data evaluation (Supplementary material 9).

The F_S reflected the chlorophyll content in cells with minor diel variation. The F_S was lower in the Sun pilot plant than in both cycles of the LED + Sun pilot plant cultivation during the first 25 days of cultivation (Supplementary material 9). The decrease of F_S in the later phases during LED + Sun cycles of the cultivation was given by lowering Chl *a* concentration during culture senescence in late stationary phase (Fig. 6). Nevertheless, the Φ_{PSII} indicated stable relatively good physiological state of all cultures with exception of several days after the dilution (Fig. 6). The algae were stressed least during the LED + Sun 2 run, but they encountered some stress during the cultivation in the Sun pilot plant (Supplementary material). The rETR was comparable in both LED + Sun cycles but was much lower during the Sun cycle due to including night phases when rETR equaled to 0 and lower irradiances during the day (Fig. 8, Supplementary material 10).

While the F_S did not show any significant diel variation in all cultivation cycles, and the range of the values reflected rather the Chl *a* content changes during the cultivation cycles (Supplementary material 11). While the Φ_{PSII} and rETR varied only slightly during the LED + Sun cycles, the pronounces diel cycles of the Φ_{PSII} and rETR were observed in the Sun cycle. The Φ_{PSII} decreased during the daylight phase of the cultivation till midday/early afternoon followed by relaxation late afternoon and reaching maximum values during the night phase. The rETR was zero during the night phase. After the sunrise, the rETR raised to its maximum around the midday and then declined to zero after the sunset (Fig. 9).

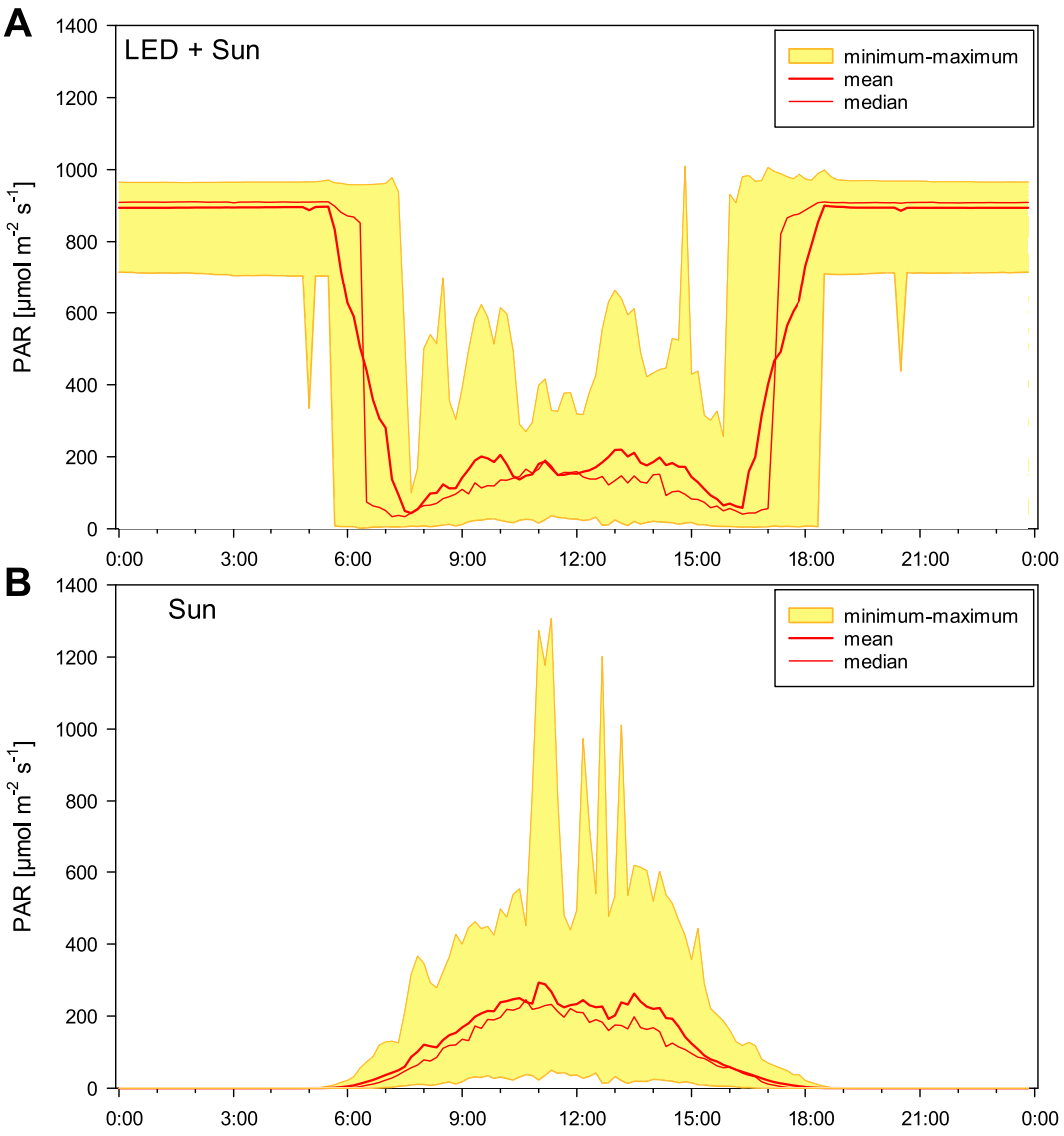

Fig. 4. The diel courses of PAR and in the (A) LED + Sun and (B) Sun pilot plants.

3.3.2. *Physiological state during cultivation*

The high values of the F_V/F_M, as well as the Φ_{PSII}, indicated very good physiological state of the alga during cultivation, only minor decrease was observed after the dilution. Although the differences in the F_V/F_M among were minor, they were still statistically significant and revealed slightly better physiological state of the cultures during the LED + Sun cycles (Table 5). Contrary to the DW production, the physiological state of the alga was better during the LED + Sun 2 cycle.

The OJIP transient parameters also indicated good physiological state of the alga. Although the LED + Sun 2 cycle showed the best parameters as in case of F_V/F_M, the physiological state and photosynthetic performance of the alga during the Sun cycle indicated less stressing conditions than during the LED + Sun 1 cycle. Significant differences were found technical parameters F_M/F_0, F_V/F_0, V_J and V_I, in quantum yields φ_{Po}, φ_{ET2o}, φ_{RE1o} and φ_{DIo}, efficiencies/probabilities Ψ_{ET2o}, Ψ_{RE1o} and δ, but in fluxes per active reaction center, only J^0_{RE1}/RC differed significantly (Supplementary material 12). The t_{Fmax} was significantly shorter in the Sun pilot plant (Supplementary material 12).

3.4. *Effects of cultivation conditions on algal growth, photosynthetic performance, and physiological state*

Due to the tight collinearity of suspension and air temperatures, and of PAR and sum of radiation, only suspension temperature, PAR and cultivation duration were considered in correlation and multivariate analyses. While in the LED + Sun cultivation cycles the $T_{suspension}$ and PAR were independent, positive correlation between these variables was found in the Sun cultivation cycle. Since the number of valid datapoints differed among the measurements, the analyses were separated according to the frequency of measurements.

Low numbers of datapoints provided by the spectrophotometric measurements compared to number of explaining (environmental) and explained (DW, Chl *a*, growth rated Chl *a*) variables led to the correlation analysis for all batches only. In the Sun pilot plant, the correlations to the environmental conditions were most significant than in the LED + Sun one (Table 6).

During the continuous measurements of F_S, Φ_{PSII} and rETR, the variability in data was caused mainly by the age of the culture explained more variability in the LED + Sun cycles, but its contribution was lower in the Sun cycle (Table 7).

As in case of the spectrophotometric data, low numbers of datapoints

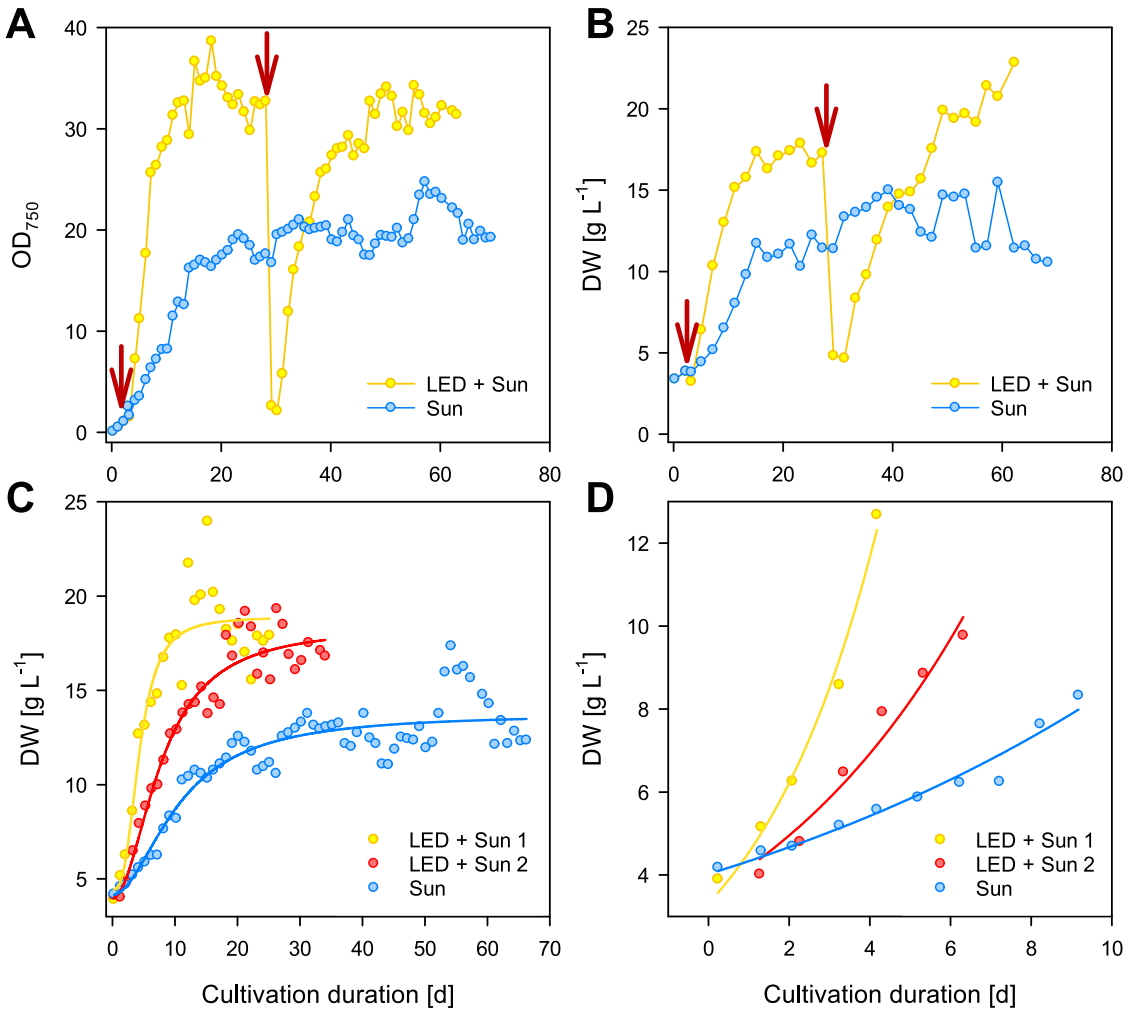

Fig. 5. The comparison of growth curves for two cultivation cycles at the LED + Sun pilot plant (LED + Sun 1 and LED + Sun 2) and one cultivation cycle at the Sun pilot plant (Sun). expressed as (A) OD_{750}, (B) DW, (C) individual cultivation cycles fitted by the logistic curve, and (D) initial part of the individual cultivation cycles fitted by the exponential phase. The red arrow indicates dilution. The dashed line represents curve fits (refer to Table 2 for the fits characteristics).

from the F_v/F_M and OJIP measurements compared to number of explaining (environmental) and explained (fluorescence) variables, only the correlation analyses could be performed. In general, the correlations of the F_V/F_M values were more profound and significant in the Sun pilot plant. No significant correlations were detected in both LED + Sun cycles with exception of the age of the culture (Table 8).

In general, the OJIP parameters were less correlated to the environmental parameters in the LED + Sun cycles than in the Sun cycle in case of technical OJIP parameters and the quantum yields (Supplementary material 13). In all cultivation cycles, only the t_{Fmax} was negatively correlated to suspension temperature significantly (Supplementary material 13a). In quantum yield and efficiencies, no significant correlation common to all cultivation was found (Supplementary material 13b) as well as in the case of fluxes per active reaction center (Supplementary material 13c).

3.5. Gross ECP production

The dry matter in the supernatants, corresponding to ECP, remained the same for the illuminated and control platform (paired *t*-test, $n = 18$, t-value = 0.5897, *P*-value = 0.563). A more substantial double increase was observed after 30 days of cultivation in both platforms, and reached 4 g L^{-1} of dry weight (Fig. 10). The dry weight of the pellet corresponded to the growth of the culture, as shown in Fig. 8.

4. Discussion

4.1. Costs & benefits of LED illumination for biomass and EPS production by D. chlorelloides

The night LED illumination of the platform resulted in huge increasement of the energy input to the cultivation resulting in slightly, but significantly, elevated cultivation temperatures due to the heat produced by the LED light sources. The input of the light energy received during the same cultivation period was ca 8× higher than in the Sun platform, reflecting thus cultivation period situated mainly after the fall equinox, expressed also as very low values of the irradiation median in the Sun pilot plant. In comparison to the similar LED illuminated photobioreactor of Schädler et al. [8], our LED illumination reached approximately half of their maximum. If considering the low-light requirements of the experimental strain [19], the lower irradiances seem to be rather beneficial. The heat input from LED light resulted also in uncoupling of the correlation between the light and temperature during the nominal diel cycles which was observed in cultivations illuminated only by the Sun (e.g. Maia et al. [42]). Since the diel cycles of temperature and light affect the cell growth, physiology and biochemistry [43–45], the effects of such PAR-temperature uncoupling should be tested during the night LED illumination.

During the cultivation, the temperature ranges in both platforms were close to growth optimum temperatures for biomass production

Table 2
The parameters of the 4-parameter logistic curve for entire cultivation and the 2-parameter exponential curve fitting parameters for its exponential phase (mean ± standard error of estimate) and the corresponding statistical data on the fitting. The number refers to the cycle number. Abbreviations: $_{est}$ = estimated, s.e. = standard error of estimate.

Pilot plant	LED + Sun 1	LED + Sun 2	Sun
Real data			
DW_{min} [g L^{-1}]	3.90	4.02	4.18
DW_{max} [g L^{-1}]	23.96	19.32	17.35
μ_{min} [d^{-1}]	−0.182	−0.151	−0.173
μ_{mean} [d^{-1}] ± s.d.	0.062 ± 0.156	0.042 ± 0.103	0.017 ± 0.072
μ_{max} [d^{-1}]	0.4193	0.2765	0.2335
AGR_{min} [g L^{-1} d^{-1}]	−3.997	−2.576	−2.281
AGR_{mean} [g L^{-1} d^{-1}] ± s.d.	0.567 ± 2.262	0.380 ± 1.355	0.133 ± 0.826
AGR_{max} [g L^{-1} d^{-1}]	6.526	3.802	2.195
Logistic curve fit			
DW_{min} [g L^{-1}] ± s.e.	4.43 ± 1.45	3.99 ± 0.83	4.15 ± 0.75
DW_{max} [g L^{-1}] ± s.e.	18.89 ± 0.681	18.40 ± 0.82	13.77 ± 0.46
t_i ± s.e.	4.296 ± 0.579	7.848 ± 0.746	10.622 ± 1.314
S ± s.e.	−2.915 ± 0.984	−2.001 ± 0.403	−1.906 ± 0.434
R^2	0.8710	0.9418	0.8398
F-value	49.50	161.9	108.3
P-value	<0.001	<0.001	<0.001
μ_{est} [d^{-1}]	0.246	0.097	0.054
AGR_{est} [g L^{-1} d^{-1}]	2.451	0.919	0.432
Initial phase			
DW_{min} [g L^{-1}] ± s.e.	3.32 ± 0.2681	3.54 ± 0.32	4.0195 ± 0.1452
μ_{est} [d^{-1}] ± s.e.	0.314 ± 0.023	0.168 ± 0.018	0.075 ± 0.009
AGR [g L^{-1} d^{-1}]	2.23	1.1422	0.4645
R^2	0.9864	0.9620	0.9590
F-value	217.9	101.4	187.1
P-value	<0.001	<0.001	<0.001

determined by the cultivation in the crossed gradients for the experimental strain determined by Kumar et al. [19]. Even the maximum temperatures did not exceed known temperature limits of growth and photosynthesis for *Dictyosphaerium*, 30–35 °C [19–21]. Even the minor difference between the temperatures in the LED + Sun and Sun platforms may still result in significant change in the importance of temperature effects on physiological performance, especially in fall-winter conditions.

In the photobioreactors, the PAR is considered as important, and often limiting, factor driving the biomass production [46,47], In our study, the PAR was found to be more important than temperature indeed. Although the mean PAR values in the Sun platform were only slightly higher than the found optima, the LED + Sun platform was exposed to 8–9× higher mean PAR [19]. Such high irradiances led to photoinhibition in the beginning of the cultivation due to lower cell densities, however at high cell densities at later stages of cultivation, the cells could be protected against the excessive light by self-shading [48], but the cell-shading in very dense suspensions could lead to light limitation as well [47].

Although receiving ca 8× more light energy, the biomass production was only 2.5× higher with night LED illumination, probably due to reaching very high cell densities in a short time leading to cell-shading and hence light limitation [47]. Nevertheless, illuminated platform was able to achieve the same biomass yield in half the time. However, when comparing to the *Microchloropsis salina* cultivation in similar photobioreactor of Schädler et al. [8], the *D. chlorelloides* biomass production in our system was lower, probably due to lower maximum irradiances compared to Schädler et al. [8] and possibly significant cell-shading effects [47]. Moreover, Schädler et al. [8] used two-stage regime with the second stage in continuous mode, while our regime consisted only from the following batch cultivations.

Contrary to biomass production, the EPS content was not affected by the light cultivation conditions. The cultivation temperatures were below the optimum for EPS production of this strain, i.e. ca 26 °C [19]. Considering the two stage cultivation proposed by Kumar et al. [19], the mass cultivation of *D. chlorelloides* should be performed in spring-early summer. For the biomass growth, lower cultivation temperatures and irradiances in spring should lead to biomass production, and their rise during early summer should stimulate the EPS production in late phases of cultivation; this hypothesis remains to be tested experimentally.

4.2. Photosynthetic activity and cultivation conditions

The values of the F_V/F_M indicated good physiological state of the cultures [14,37,38], especially when considering that measurements had been performed after local mid-day at time when the maximum stress conditions should be expected. These values are comparable to other green algae in mass cultivations [49,50], and differences in the higher or lower values could be caused by the experimental conditions (e.g. Vonshak et al. [18]).

In the Sun pilot plant, the continuously monitored fluorescence parameters Φ_{PSII} and rETR followed the diel L/D cycle as in other studies [18,51]. The continuous fluorescence measurements proved no significant photoinhibition of *D. chlorelloides* during the night LED illumination, despite of the requirement for low light of the experimental strain [19], and the lower values in the beginning of the cultivation could confirm the hypothesis of at least partial photoinhibition in the early

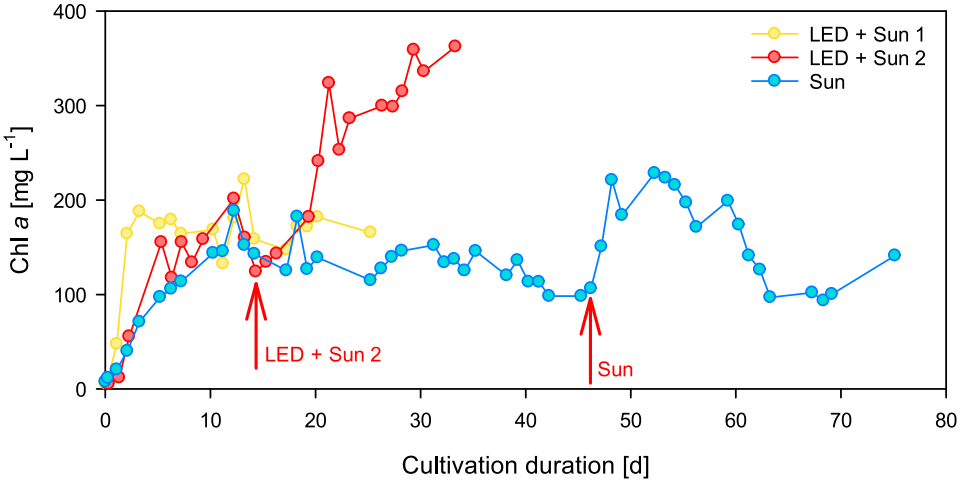

Fig. 6. The change of the chlorophyll *a* content (Chl *a*) during the individual cultivation cycles. The arrow indicates nutrient additions and the label cultivation cycle to which the nutrients were added.

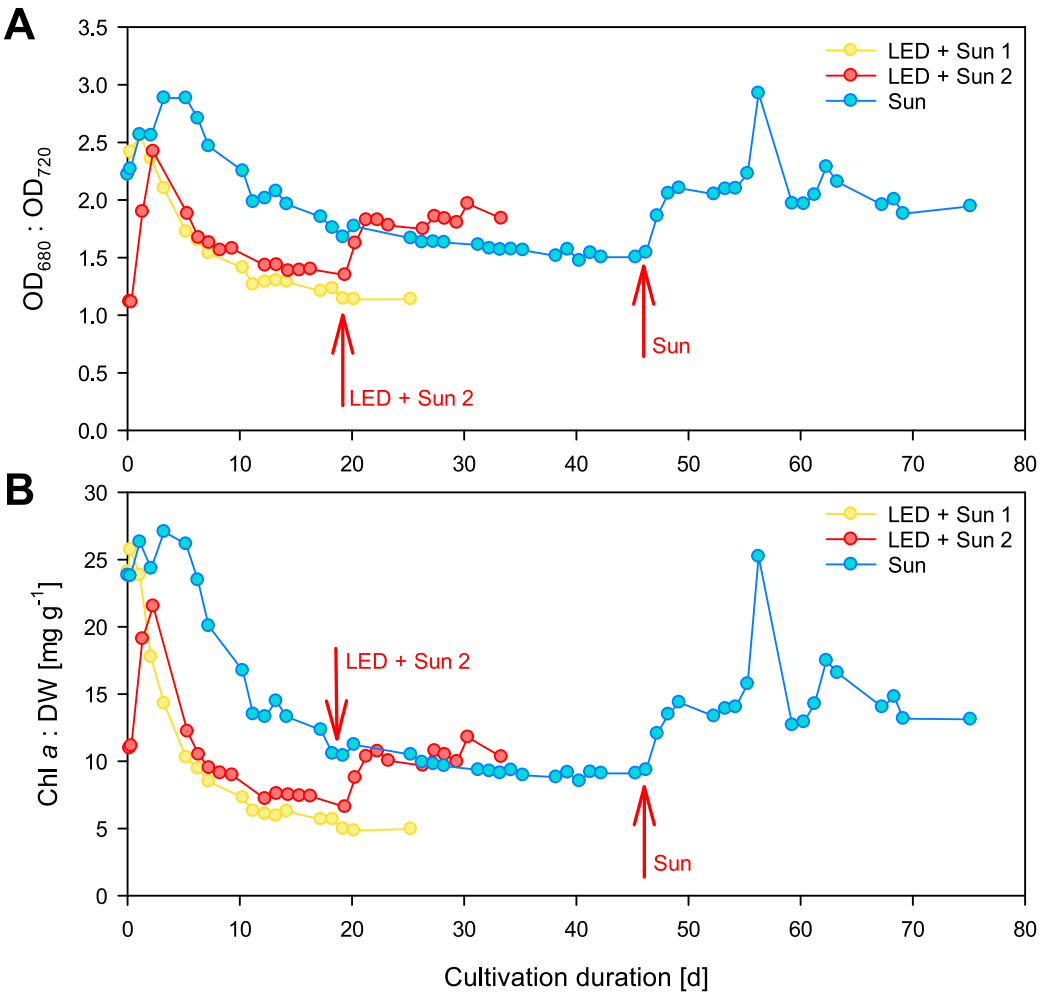

Fig. 7. The change of the (A) Chl *a*: DW ratio and (B) OD_{680} : OD720 during the individual cultivation cycles. The arrow indicates nutrient additions and the label cultivation cycle to which the nutrients were added.

Table 3
The summary characteristics of the OD_{680} : OD_{720} and Chl *a* : DW and ratios in individual pilot plants and batches.

Pilot plant	LED + Sun 1	LED + Sun 2	Sun
OD_{680} : $OD_{720\ min}$	1.137	1.114	1.474
OD_{680} : OD_{720} mn ± s.d.	1.610 ± 0.496	1.655 ± 0.289	1.973 ± 0.389
OD_{680} : $OD_{720\ max}$	2.561	2.422	2.885
Chl *a* : DW_{min}	4.85	6.61	8.53
Chl *a* : DW_{mn} ± s.d.	10.67 ± 7.25	10.39 ± 3.37	14.23 ± 5.44
Chl *a* : DW_{max}	25.75	21.55	27.07

stages of the cultivation and high-light limitation discussed above. Therefore, the maximum photosynthetic activity expressed as rETR occurred during the night in the LED + Sun pilot plant, reducing thus respiration losses [9].

Being widely-used fast and effective method for stress evaluation in plants [52], the OJIP transient was proposed for as the second method for monitoring of the physiological state of the cultures. The OJIP parameters were less affected by temperature and light in the LED + Sun pilot plant. However, the response was not consisted in both LED + Sun cultivation cycles, and they were different from the Sun cultivation cycle. Detailed experiments analysis focused on the effects of individual environmental factors should be performed to decipher the response of the OJIP parameters in *D. chlorelloides*.

4.3. Suitable parameters for automatic regulations

The OD_{750}/OD_{720} as biomass and OD_{680} as Chl *a* proxies are used regularly in algal cultivations [12,49]. However, the ratio Chl *a*/DW, tightly correlated to OD_{680}/OD_{720}, not used often in algal mass cultivation [53]. The parameter precedes the inflection point of the growth

Table 4
Comparison of dry matter production and costs for electricity, at the control (only Sun) and illuminated (LED + Sun) units, at the end of the exponential and reaching the stationary phase, the first cycle of cultivation.

Cultivation cycle	Phase	Duration days	DW production (g m^{-2} d^{-1})	DW production (g L^{-1} d^{-1})	Power consumption (kWh g^{-1})
LED + Sun 1	Exponential	16	13.55	0.11	0.22
	Linear	12	7.71	0.06	0.19
LED + Sun 2	Linear	24	11.90	0.10	0.40
Sun	Exponential	16	9.15	0.07	
	Linear	42	4.46	0.04	

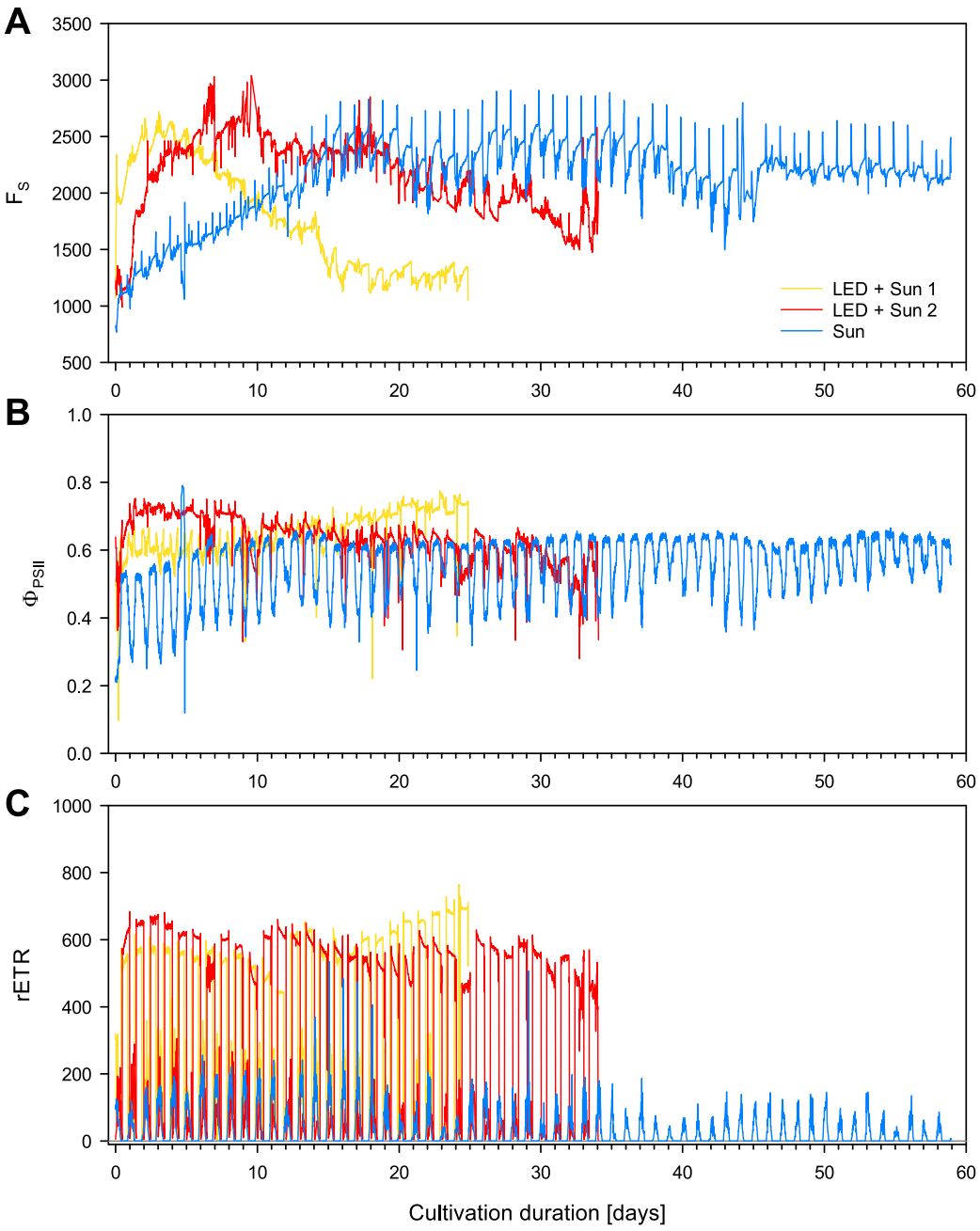

Fig. 8. The course of (A) steady-state fluorescence in light (F_S), (B) effective quantum yield (Φ_{PSII}) and (C) relative electron transport rate (rETR) during cultivation in the LED and Sun pilot plants.

curve by 3–4 days, therefore should be used as marker of change in the cultivation conditions [35,36], in our case probably nutrient limitation as nutrient addition led to increase of this parameter. The difference in this parameter between the LED + Sun and the Sun cycles was caused probably by different light conditions [53].

The F_V/F_M is commonly used for physiological state evaluation (e.g. Malapascua et al. [14]) and could be used with other parameters for estimation of production of valuable compounds [54]. The F_0 was found even as good Chl *a* proxy [55], however this measurement requires defined dark adaptation which cannot be performed easily in automated system. The continuous in situ variable chlorophyll fluorescence monitoring, especially in continuous light, is affected inevitably by light at least (e.g. Roháček et al. [38]), but it could be used for more frequent measurements. Parameters Φ_{PSII} and rETR revealed the stability of the photosynthetic activity in the LED + Sun pilot plant. Such data should be used to determine optimal illumination of the unit to keep rETR, and hence the biomass production at its maximum. The decrease in Φ_{PSII} and rETR should indicate deteriorating growth conditions (e.g. Roháček et al. [38]), or the pre-defined decreased values could be used as parameter for optimization of secondary metabolite production [54]. In our case, this system should be applied in Sun pilot plant, where significant correlations between growth and fluorescence parameters had been detected. Contrary in the LED + Sun pilot plant, these correlations were not so significant, probably due to the more suitable cultivation conditions.

For detailed regulation of the cultivation, both spectrophotometric and fluorescence parameters should be applied. In the biomass growth phase, the rate of biomass production and optimum conditions should lead to exponential growth. For production, the growth conditions should be manipulated to keep stationary phase and pre-defined level of

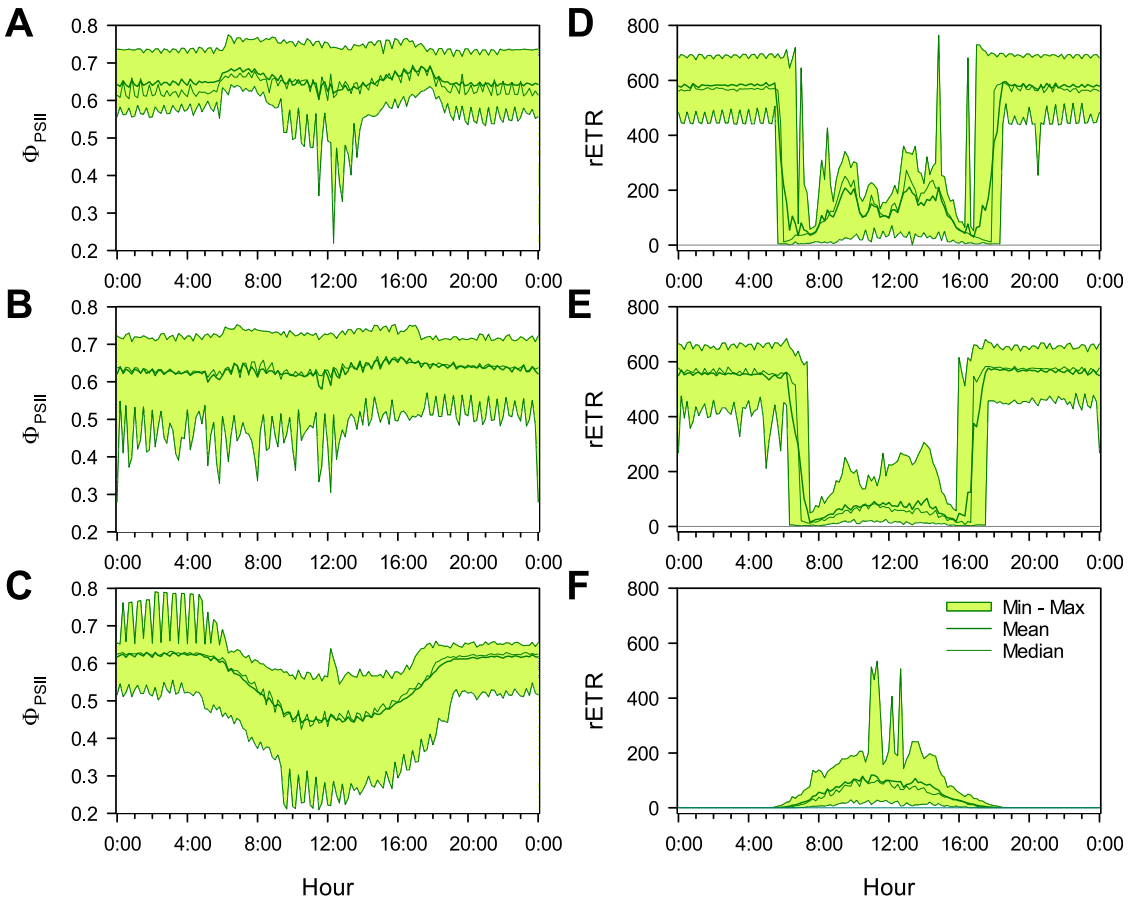

Fig. 9. Diel variation in the effective quantum yield (Φ_{PSII}) during (A) LED + Sun 1 cycle, (B) LED + Sun 2 cycle and (C) Sun cycle, and in the relative electron transport rate (rETR) during (D) LED + Sun 1 cycle, (E) LED + Sun 2 cycle and (F) Sun cycle.

Table 5
Comparison of the F_V/F_M values during the first 25 days of cultivation (mean ± standard deviation, Friedmann ANOVA for dependent samples test, $n = 14$). The first day of the cultivation was not included in the analysis. The number in subscript indicates cultivation duration in days and $_{total}$ states entire cultivation duration. The statistically significant differences are marked in bold.

	LED + Sun 1	LED + Sun 2	Sun	ANOVA χ^2-value	P-value
F_V/F_M	0.772 ± 0.020	0.798 ± 0.041	0.754 ± 0.038	**11.82**	**0.003**
F_V/F_M min	0.739	0.667	0.653		
F_V/F_M max	0.805	0.832	0.808		

stress to maximize secondary metabolites production. Additional spectrophotometric measurements using hyperspectral camera should improve the regulation processes [56,57].

4.4. Electricity costs

Finally, the electricity consumption in the LED + Sun 1 was 35.7–40 kWh per night in the LE + Sun 1 cycle and increased to 58.2 kWh per night, due to night prolongation from September to November and variable light conditions during these days, resulting in energy consumptions of 0.20 and 0.41 kWh g^{-1} DW. The differences reflected probably the night prolongation during the fall. These values of energy consumption in the LED + Sun 1 cultivations are comparable to other experiments but were higher in the LED + Sun 2 cycle. Abomohra et al. [58] reported energy consumption for night LED illumination of ca 0.2 kWh g^{-1} DW for green alga *Scenedesmus obliquus* and these data are similar to Blanken et al. [11]. However, Abomohra et al. [58] used different light regime of 12 h. of constant white light/4 h of dark/8 h od monochromatic light, and the mean LED irradiances were about 150 μmol.m^{-2}.s^{-1}, while in our experiments, the Sun/LED regime ranged from 13.3/10.7 at the beginning of the cultivation to 9.7/13.3 at its end, and the LED provided ca 850–900 μmol.m^{-2}.s^{-1}, resulting thus in higher electricity consumption. Therefore, the natural diel light cycle should be considered in estimation of energy costs for biomass production, especially in higher latitudes.

5. Conclusions

The night LED illumination increased the biomass production and by the productivity of the alga *Dictyosphaerium chlorelloides* by about 2.5× (6150 g/8.542 g DW m^{-2} d^{-1}/0.683 g DW L^{-1} d^{-1}) compared to the sun illuminated pilot plants (2400 g/3.333 g DW m^{-2} d^{-1}/0.267 g DW L^{-1} d^{-1}), demonstrating thus the possibility of successful algal cultivation even in fall-winter time in the temperate zone. The combination of spectrophotometric and fluorometric measurements led to detailed information on algal growth and physiological state, and was used later for nutrient additions in stationary phase leading to increased growth. In the LED + Sun, the effective quantum yield was stable during the day, in average ca 0.65, while significant drop to ca 0.45 was observed in the Sun pilot plant at midday, contributing to significantly lower mean maximum quantum yield of 0.754 in the Sun pilot pant compared to the LED + Sun pilot plant (0.784). Nevertheless, the maximum quantum yield values indicated good physiological state of the alga in both platforms. Although the basic fluorescence parameters maximum and

Table 6
The heatmap of correlations between the environmental variables and dry weight, Chl *a*, growth rates, Chl *a*: DW ratio and its change. The color scale indicates the r-value: red – $r = -1$, white = $r = 0$, green – $r = 1$. The statistically significant correlations are marked in bold. Abbreviations: DW – dry weight, AGR_{DW} – absolute growth rate based on dry weight, μ_{DW} – relative growth rate based on dry weight, Chl *a* – chlorophyll *a*, $AGR_{Chl\ a}$ – absolute growth rate per day based on Chl *a*, μChl a – relative growth rate per day based on Chl *a*, Chl *a*:DW – ratio between Chl *a* and DW, ΔChl *a*:DW – diel change of the Chl *a*:DW ratio.

		$T_{suspension}$			PAR			Sum of
	Age	mean	minimum	maximum	mean	minimum	maximum	radiation
LED +Sun 1								
DW	**0.8809**	-0.4249	-0.3271	-0.4114	**-0.5194**	-0.2415	**-0.6525**	**-0.572**
AGR_{DW}	-0.1501	0.4384	0.4922	0.3247	-0.3329	-0.4935	-0.3989	-0.3273
μ_{DW}	**-0.5815**	0.4267	0.4051	0.3314	0.291	0.1236	0.2416	0.1105
Chl *a*	0.2976	-0.0968	0.078	-0.192	-0.476	-0.3672	-0.4692	-0.4429
$AGR_{Chl\ a}$	-0.3533	0.392	0.4945	0.2153	-0.0029	-0.1493	-0.0966	-0.2313
$\mu_{Chl\ a}$	**-0.5177**	0.369	0.3153	0.3114	0.2652	0.1484	0.2285	0.14
Chl *a*:DW	**-0.8067**	0.4183	0.3722	0.3639	0.386	0.1791	0.5012	0.4124
ΔChl *a*:DW	**0.7105**	-0.3916	**-0.5003**	-0.204	-0.4448	-0.1476	-0.4292	-0.1454
LED +Sun 2								
DW	**0.9172**	**-0.4352**	-0.116	-0.3745	0.3196	**-0.4443**	0.1111	0.3214
AGR_{DW}	-0.073	0.274	0.1785	0.2746	-0.2135	0.0679	-0.3896	0.0277
μ_{DW}	-0.1565	0.3212	0.2461	0.202	-0.1184	0.0394	-0.3427	-0.0564
Chl *a*	**0.9379**	-0.292	0.0165	-0.2748	0.3663	**-0.501**	0.1705	0.3674
$AGR_{Chl\ a}$	0.03	0.1706	0.1153	0.2158	-0.2971	-0.1159	-0.3778	-0.0702
$\mu_{Chl\ a}$	-0.1743	0.3086	0.1451	0.2113	-0.0692	0.0491	-0.2378	-0.0687
Chl *a*:DW	-0.3413	**0.5347**	0.265	0.4337	0.1053	0.1123	0.1641	0.0288
ΔChl *a*:DW	-0.1641	0.1212	-0.1926	0.1268	0.1049	0.094	0.2068	-0.0437
Sun								
DW	**0.4433**	**-0.33**	**-0.3315**	-0.2303	**-0.3307**	n/a	-0.1707	**-0.3315**
AGR_{DW}	**-0.3333**	**0.3202**	0.1913	**0.3827**	**0.4024**	n/a	0.2821	**0.4219**
μ_{DW}	**-0.575**	**0.5438**	**0.468**	**0.563**	**0.4862**	n/a	**0.3085**	**0.4997**
Chl *a*	**0.499**	-0.2142	-0.2238	-0.1439	**-0.2695**	n/a	-0.1845	-0.2602
$AGR_{Chl\ a}$	-0.2777	0.2697	0.1769	**0.3325**	**0.3312**	n/a	0.218	**0.3493**
$\mu_{Chl\ a}$	**-0.483**	**0.4629**	**0.4279**	**0.4744**	**0.3905**	n/a	0.2075	**0.4059**
Chl *a*:DW	**-0.3485**	**0.3949**	**0.3851**	**0.3213**	**0.3402**	n/a	0.1669	**0.3589**
ΔChl *a*:DW	**0.3139**	**-0.2999**	-0.2255	**-0.3217**	-0.271	n/a	-0.2262	-0.267

Table 7
The contributions of individual environmental variables to the observed variability in continuously monitored fluorescence parameters F_S, Φ_{PSII} and rETR.

	Variable	Explains %	Contribution %	Pseudo-F	P-value
LED + Sun 1	Age	51.1	59.0	2476	0.002
	PAR	33.5	38.6	5149	0.002
	$T_{suspension}$	2.0	2.4	363	0.002
LED + Sun 2	PAR	32.6	59.2	1569	0.002
	Age	21.6	39.3	1533	0.002
	$T_{suspension}$	0.8	1.4	57.4	0.002
Sun	PAR	55.4	82.8	6960	0.002
	$T_{suspension}$	8.4	12.5	1297	0.002
	Age	3.1	4.7	533	0.002

effective quantum yields could be used in both light regimes, different sets of parameters sets of fluorescence transient parameters must be suggested. The electricity costs ranging from 0.20 to 0.41 kWh g^{-1} DW were higher than in other studies and the reflected the prolonged LED light period and higher irradiances provided by the LED light source.

Supplementary data to this article can be found online at https://doi.org/10.1016/j.algal.2024.103759.

CRediT authorship contribution statement

Jana Kvíderová: Conceptualization, Data curation, Investigation, Methodology, Resources, Software, Validation, Visualization, Writing – original draft, Writing – review & editing. **David Kubáč:** Investigation, Methodology, Writing – original draft. **Jaromír Lukavský:** Conceptualization, Data curation, Funding acquisition, Investigation, Methodology, Project administration, Resources, Supervision, Validation, Writing – original draft.

Declaration of competing interest

The authors declare that they have no known competing financial interests or personal relationships that could have appeared to influence the work reported in this paper.

Table 8
The heatmap of correlation coefficient values (r) of the correlation analysis between the F_V/F_M and the environmental variables in all cultivation cycles. The color scale indicates the r-value: red – $r = -1$, white = $r = 0$, green – $r = 1$. The statistically significant correlations are marked in bold.

		$T_{suspension}$			PAR			Sum of
Cycle	Age	mean	minimum	maximum	mean	minimum	maximum	radiation
LED + Sun 1	0.2621	-0.1182	0.3803	-0.4373	-0.1506	0.1174	-0.2643	-0.4192
LED + Sun 2	**0.4747**	-0.3342	-0.1214	-0.3774	0.0474	-0.3779	-0.2295	-0.018
Sun	**0.75**	**-0.5453**	**-0.3876**	**-0.5178**	**-0.6813**	n/a	**-0.502**	**-0.6734**

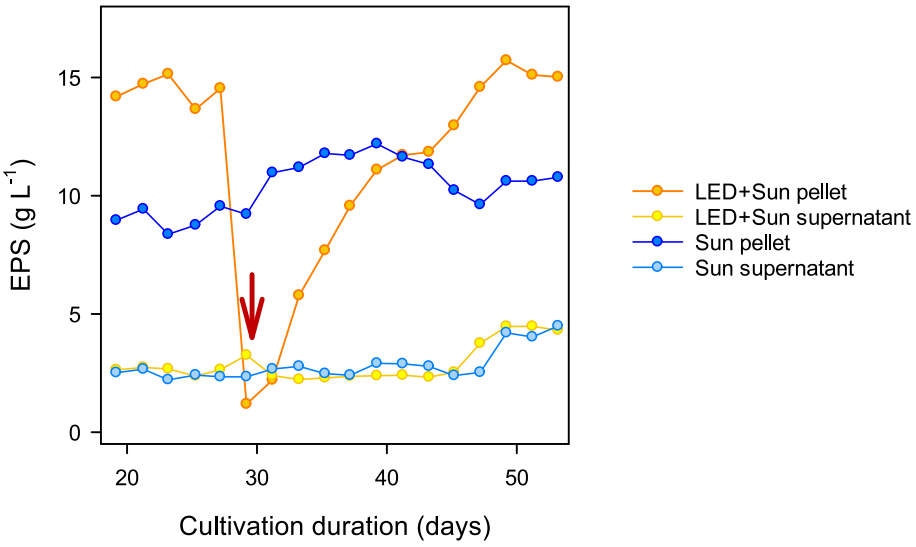

Fig. 10. Growth curves of the alga *Dictyosphaerium chlorelloides* where the dry matter of sediment and supernatant was measured after centrifugation separately. The arrow indicates dilution before the second cultivation cycle in the LED + Sun pilot plant.

Data availability

Data will be made available on request.

Acknowledgements

The work was supported by projects Technology Agency of the Czech Republic [TN 01000048], institutional long-term research plan of the Czech Academy of Sciences [RVO67985939] and The Ministry of Education, Youth and Sports of the Czech Republic [LTAIN 19139].

Last not least we would like to thank prof. J.D. Brooker for language dressing and Hana Brabcová for technical support.

References

[1] M.A. Borowitzka, High-value products from microalgae—their development and commercialisation, J. Appl. Phycol. 25 (3) (2013) 743–756.
[2] O. Pulz, W. Gross, Valuable products from biotechnology of microalgae, Appl. Microbiol. Biotechnol. 65 (2004) 635–648.
[3] A. Perosa, et al., Algae as a Potential Source of Food and Energy in Developing Countries: Sustainability, Technology and Selected Case Studies, Edizioni Ca'Foscari-Digital Publishing, Venezia, 2015, p. 130.
[4] J.U. Grobbelaar, L. Nedbal, V. Tichy, Influence of high frequency light/dark fluctuations on photosynthetic characteristics of microalgae photoacclimated to different light intensities and implications for mass algal cultivation, J. Appl. Phycol. 8 (4–5) (1996) 335–343.
[5] L. Nedbal, et al., A photobioreactor system for precision cultivation of photoautotrophic microorganisms and for high-content analysis of suspension dynamics, Biotechnol. Bioeng. 100 (5) (2008) 902–910.
[6] M. Sergejevová, et al., Photobioreactors with internal illumination, in: A. Prokop, R.K. Bajpai, M.E. Zappi (Eds.), Algal Biorefineries: Volume 2: Products and Refinery Design, Springer International Publishing, Cham, 2015, pp. 213–236.
[7] M. Glemser, et al., Application of light-emitting diodes (LEDs) in cultivation of phototrophic microalgae: current state and perspectives, Appl. Microbiol. Biotechnol. 100 (3) (2016) 1077–1088.
[8] T. Schädler, et al., Continuous production of lipids with Microchloropsis salina in open thin-layer cascade photobioreactors on a pilot scale, Energies 14 (2) (2021) 500.
[9] S.J. Edmundson, M.H. Huesemann, The dark side of algae cultivation: characterizing night biomass loss in three photosynthetic algae, Chlorella sorokiniana, Nannochloropsis salina and Picochlorum sp, Algal Res. 12 (2015) 470–476.
[10] J. Kvíderová, et al., Perspectives of low-temperature biomass production of polar microalgae and biotechnology expansion into high latitudes, in: R. Margesin (Ed.), Psychrophiles: From Biodiversity to Biotechnology, Springer, Cham, 2017, pp. 585–600.
[11] W. Blanken, et al., Cultivation of microalgae on artificial light comes at a cost, Algal Res. 2 (4) (2013) 333–340.
[12] R.A. Andersen, Algal Culturing Techniques, Elsevier Academic Press, Amsterdam, Boston, Heidelberg, London, New York, Oxford, San Diego, San Francisco, Singapore, Sydney, Tokyo, 2005, p. 578.
[13] J. Masojídek, A. Vonshak, G. Torzillo, Chlorophyll fluorescence applications in microalgal mass cultures, in: D.J. Suggett, O. Prášil, M.A. Borowitzka (Eds.), Chlorophyll a Fluorescence in Aquatic Sciences: Methods and Applications, Springer, Dordrecht Heidelberg London New York, 2010, pp. 277–292.
[14] J.R. Malapascua, et al., Photosynthesis monitoring to optimize growth of microalgal mass cultures: application of chlorophyll fluorescence techniques, Aquat. Biol. 22 (2014) 123–140.
[15] K. Ranglová, et al., Rapid screening test to estimate temperature optima for microalgae growth using photosynthesis activity measurements, Folia Microbiol. 64 (5) (2019) 615–625.
[16] G. Torzillo, et al., In situ monitoring of chlorophyll fluorescence to assess the synergistic effect of low temperature and high irradiance stresses in Spirulina cultures grown outdoors in photobioreactors, J. Appl. Phycol. 8 (4–5) (1996) 283–291.
[17] G. Torzillo, P. Bernardini, J. Masojídek, On-line monitoring of chlorophyll fluorescence to assess the extent of photoinhibition of photosynthesis induced by high oxygen concentration and low temperature and its effect on the productivity of outdoor cultures of Spirulina platensis (Cyanobacteria), J. Phycol. 34 (1998) 504–510.

[18] A. Vonshak, et al., Sub-optimal morning temperature induces photoinhibition in dense outdoor cultures of the alga Monodus subterraneus (Eustigmatophyta), Plant Cell Environ. 24 (10) (2001) 1113–1118.
[19] D. Kumar, et al., The green alga Dictyosphaerium chlorelloides biomass and polysaccharides production determined using cultivation in crossed gradients of temperature and light, Eng. Life Sci. 17 (9) (2017) 1030–1038.
[20] I.E. Huertas, et al., Warming will affect phytoplankton differently: evidence through a mechanistic approach, Proc. R. Soc. Lond. B Biol. Sci. 278 (1724) (2011) 3534–3543.
[21] A. Sánchez-Fortún Herrero, Influencia de factores externos sobre la fotosíntesis de algas verdes y cianobacterias [Influence of external factors on photosynthesis of green algae and cyanobacteria], REDUCA 6 (4) (2014) 32–38.
[22] M.B. Fard, D. Wu, Potential interactive effect on biomass and bio-polymeric substances of microalgal-bacterial aerobic granular sludge as a valuable resource for sustainable development, Bioresour. Technol. 376 (2023) 128929.
[23] A. Synytsya, et al., Chapter 8 - intracellular and extracellular carbohydrates in microalgae, in: E. Jacob-Lopes, et al. (Eds.), Handbook of Food and Feed from Microalgae, Academic Press, 2023, pp. 87–102.
[24] M.C. Deprá, et al., Bioactive polysaccharides from microalgae: a close look at the biomedical applications, Recent Pat. Biotechnol. 17 (4) (2023) 296–311.
[25] M.B.F. da Silva, C.M.L.L. Teixeira, Cyanobacterial and microalgae polymers: antiviral activity and applications, Braz. J. Microbiol. (2024) 1–15.
[26] M. Franco-Morgado, et al., Microalgae and cyanobacteria polysaccharides: important link for nutrient recycling and revalorization of agro-industrial wastewater, Appl. Food Res. 3 (1) (2023) 100296.
[27] M. Halaj, et al., Chemico-physical and pharmacodynamic properties of extracellular Dictyosphaerium chlorelloides biopolymer, Carbohydr. Polym. 198 (2018) 215–224.
[28] M. Halaj, et al., Biopolymer of Dictyosphaerium chlorelloides - chemical characterization and biological effects, Int. J. Biol. Macromol. 113 (2018) 1248–1257.
[29] M. Halaj, et al., Extracellular biopolymers produced by Dictyosphaerium family - chemical and immunomodulative properties, Int. J. Biol. Macromol. 121 (2019) 1254–1263.
[30] M. Matulová, P. Capek, Structural properties of the biologically active Dictyosphaerium chlorelloides exopolysaccharide α-d-manno-α-l-rhamno-α-d-(2-O-methyl)-galactan, Carbohydr. Res. 534 (2023) 108946.
[31] V. Zachleder, I. Šetlík, Efect of irradiance on the course of RNA synthesis in the cell cycle of Scenedesmus quadricauda, Biol. Plant. 24 (5) (1982) 341–353.
[32] H.C. Venancio, et al., Surface-to-volume ratio influence on the growth of Scenedesmus obliquus in a thin-layer cascade system, J. Appl. Phycol. 32 (2) (2020) 821–829.
[33] Doucha, J. and K. Lívanský, The way of outdoor thin-layer cultivation of algae and blue-green algae and bioreactor for carrying out this method. 1996. CZ patent 3266-96, CZ 9966U1.
[34] J. Kvíderová, W.J. Henley, The effect of ampicillin plus streptomycin on growth and photosynthesis of two halotolerant chlorophyte algae, J. Appl. Phycol. 17 (2005) 301–307.
[35] Y. Li, et al., Effects of nitrogen sources on cell growth and lipid accumulation of green alga Neochloris oleoabundans, Appl. Microbiol. Biotechnol. 81 (2008) 629–636.
[36] R.J. Geider, H.L. MacIntyre, T.M. Kana, A dynamic regulatory model of phytoplanktonic acclimation to light, nutrients, and temperature, Limnol. Oceanogr. 43 (4) (1998) 679–694.
[37] K. Maxwell, G.N. Johnson, Chlorophyll fluorescence - a practical guide, J. Exp. Bot. 51 (345) (2000) 659–668.
[38] K. Roháček, J. Soukupová, M. Barták, Chlorophyll fluorescence: a wonderful tool to study plant physiology and plant stress, in: B. Schoefs (Ed.), Plant Cell Compartments-Selected Topics, Research Signpost, Kerala, India, 2008, pp. 41–104.
[39] A. Stibert, et al., Chlorophyll a fluorescence induction in higher plants: modelling and numerical simulatioj, J. Theor. Biol. 193 (1998) 131–151.
[40] R.J. Strasser, M. Tsimilli-Michael, A. Srivastava, Analysis of the chlorophyll a fluorescence transient, in: G.C. Papageorgiou, Govindjee (Eds.), Chlorophyll A Fluorescence: A Signature of Photosynthesis, Springer, Dordrecht, 2004, pp. 321–362.
[41] C.J.F. Ter Braak, P. Šmilauer, Canoco Reference Manual and User's Guide: Software for Ordination, Version 5.0, Microcomputer Power, Ithaca, USA, 2012, p. 496.
[42] I.B. Maia, et al., Diel biochemical and photosynthetic monitorization of Skeletonema costatum and Phaeodactylum tricornutum grown in outdoor pilot-scale flat panel photobioreactors, J. Biotechnol. 343 (2022) 110–119.
[43] B. Tamburic, et al., The effect of diel temperature and light cycles on the growth of Nannochloropsis oculata in a photobioreactor matrix, PloS One 9 (1) (2014) e86047.
[44] S. Srirangan, et al., Interaction of temperature and photoperiod increases growth and oil content in the marine microalgae Dunaliella viridis, PloS One 10 (5) (2015) e0127562.
[45] M. Ras, J.-P. Steyer, O. Bernard, Temperature effect on microalgae: a crucial factor for outdoor production, Rev. Environ. Sci. Bio-Technol. 12 (2) (2013) 153–164.
[46] O. Pulz, K. Scheibenbogen, Photobioreactors: design and performance with respect to light energy input, in: T. Scheper (Ed.), Bioprocess and Algae Reactor Technology, Apoptosis, Springer Berlin Heidelberg, Berlin, Heidelberg, 1998, pp. 123–152.
[47] E. Sforza, et al., Adjusted light and dark cycles can optimize photosynthetic efficiency in algae growing in photobioreactors, PloS One 7 (6) (2012) e38975.
[48] R. Sommaruga, Y. Chen, Z. Liu, Multiple strategies of bloom-forming Microcystis to minimize damage by solar ultraviolet radiation in surface waters, Microb. Ecol. 57 (4) (2009) 667–674.
[49] A. Solovchenko, et al., Phycoremediation of alcohol distillery wastewater with a novel Chlorella sorokiniana strain cultivated in a photobioreactor monitored on-line via chlorophyll fluorescence, Algal Res. 6 (2014) 234–241.
[50] A. Jebali, et al., Evaluation of native microalgae from Tunisia using the pulse-amplitude-modulation measurement of chlorophyll fluorescence and a performance study in semi-continuous mode for biofuel production, Biotechnol. Biofuels 12 (1) (2019) 119.
[51] R. Barten, et al., Towards industrial production of microalgae without temperature control: the effect of diel temperature fluctuations on microalgal physiology, J. Biotechnol. 336 (2021) 56–63.
[52] B.J. Strasser, A. Srivastava, M. Tsimilli-Michael, The fluorescence transient as a tool to characterize and screen photosynthetic samples, in: M. Yunus, U. Pathre, P. Mohanty (Eds.), Probing Photosynthesis: Mechanisms, Regulation and Adaptation, Taylor & Francis, London, 2000, pp. 445–483.
[53] J.C. Kromkamp, et al., Short-term variations in photosynthetic parameters of Nannochloropsis cultures grown in two types of outdoor mass cultivation systems, Aquat. Microb. Ecol. 56 (2–3) (2009) 309–322.
[54] S.H. Oh, Y.K. Chang, J.H. Lee, Identification of significant proxy variable for the physiological status affecting salt stress-induced lipid accumulation in Chlorella sorokiniana HS1, Biotechnol. Biofuels 12 (2019) 1–13.
[55] C. Honeywill, D.M. Paterson, S.E. Hagerthey, Determination of microphytobenthic biomass using pulse-amplitude modulated minimum fluorescence, Eur. J. Phycol. 37 (4) (2002) 485–492.
[56] P. Salmi, et al., Rapid quantification of microalgae growth with hyperspectral camera and vegetation indices, Plants 10 (2) (2021) 341.
[57] K.B. Mishra, P. Vítek, M. Barták, A correlative approach, combining chlorophyll a fluorescence, reflectance, and Raman spectroscopy, for monitoring hydration induced changes in Antarctic lichen Dermatocarpon polyphyllizum, Spectrochim. Acta A Mol. Biomol. Spectrosc. 208 (2019) 13–23.
[58] A.E.-F. Abomohra, et al., Night illumination using monochromatic light-emitting diodes for enhanced microalgal growth and biodiesel production, Bioresour. Technol. 288 (2019) 121514.